Power Performance Enhancement of Underlay Spectrum Sharing in Cognitive Radio Networks Using ESPAR Antenna

Ahmad ABDALRAZIK*, Heba SOLIMAN, Mohamed ABDELKADER
Port Said University, Faculty of Engineering, Port Said, Egypt
ahmadabdalrazik@eng.psu.edu.eg

***Abstract*—Electronically-steerable parasitic array radiator (ESPAR) antenna is a promising antenna array configuration. It offers lower power consumption, lower cost, lower hardware complexity, and smaller size as compared to classical antenna arrays configurations. Meanwhile it is able to support important communication techniques such as beamforming and diversity. In this paper, we propose a transmitter ESPAR antenna system where symbols are transmitted over switchable beampatterns of the antenna in order to enhance the power performance of underlay spectrum sharing in cognitive radio networks compared to previously proposed transmitter systems. We study the performance of two different pattern shapes of ESPAR antenna to choose the appropriate one for underlay spectrum sharing. We show through simulation that the ESPAR antenna can offer a better power performance than a classical circular antenna array (CAA) of the same size and comparable number of elements. In addition, the ESPAR antenna can preserve its good performance with small spacing between elements, whereas the classical CAA's performance severely degrades.**

***Index Terms*—antenna arrays, antenna radiation patterns, cognitive radio, MATLAB, multipath channels.**

I. INTRODUCTION

Cognitive radio networks (CRN) have been widely considered as an auspicious solution for the growing problem of spectrum scarcity. Studies of the Federal Communication Commission (FCC) have shown that a large portion of the licensed bandwidth is underutilized. In CRN, secondary users (SUs) can transmit data within the same band of licensed primary users (PUs), provided that interference levels at the PUs are within pre-defined limits. SU's transmission of data can occur either concurrently while PUs are communicating (underlay spectrum sharing) or when PUs are silent (overlay spectrum sharing) [1].

In the literature, underlay spectrum sharing has been achieved using conventional antenna arrays through transmitting weighted versions of a symbol over statistically independent channels [2-4]. The precoding weight vector is optimized such that it maximizes the transmitted power to the SU receiver (SU-Rx) while keeping transmitted power to PU receiver (PU-Rx) under a certain limit.

However, conventional antenna arrays need complex design requirements [5]. They require an individual RF chain to be connected to each of the array elements. Moreover, isolators and sufficient separation between elements are necessary to reduce mutual coupling between the elements. This has motivated the need for novel antenna array configurations that impose less hardware complexity, power consumption, cost, and antenna size.

Electronically-steerable parasitic array radiator (ESPAR) antenna [6] is considered as a promising configuration of antenna arrays and has received increasing attention lately. It has been used to attain lower power consumption, lower cost, lower complexity, and smaller size as compared to conventional antenna arrays [7-10]. It consists of one active element and multiple passive elements mutually-coupled to the active one. This mutual coupling is created by reducing the spacing between the elements of the ESPAR antenna array, which gives it the advantage of small size and eliminates the need for isolators between elements. The active element is connected to the receiver/transmitter circuit and the passive elements are reactively loaded. Hence, it needs only one RF chain, which considerably reduces the power consumption, cost, and hardware complexity needed. In this paper, we will focus on the ESPAR antenna's ability to enhance power performance of underlay spectrum sharing while working properly under small size restrictions.

Contrarily to conventional antenna arrays, ESPAR antenna elements cannot serve directly as individual receive/transmit branches. This is simply because only one of the ESPAR antenna elements is connected to the RF chain. Despite this limitation, ESPAR antennas were used to achieve receive diversity though using switchable beampatterns of the antenna as individual receive branches in [9] and [10]. Also, receive beamforming has been achieved using ESPAR antenna to maximize the received signal while minimizing the interference [11-13]. In addition, it was used for spectrum sensing in cognitive radio networks [14-15].

In the context of underlay spectrum sharing, an ESPAR antenna has been used in [16] to form a power pattern of the SU transmitter with nulls towards the PU receivers. However, issues like maximizing antenna efficiency and maximizing transmitted power towards SU receivers were not considered. Maximizing transmitted power to SU receivers is specifically important for stationary and power limited devices. More recently, the authors of [17] have proposed an algorithm to maximize the transmitted power to SU receivers, while minimizing interference to PU receivers. However, a line-of-sight communication was implicitly assumed. Moreover, it was assumed that the directions of the PU and SU receivers are known apriori.

In this paper, we propose a transmitter ESPAR antenna system for underlay spectrum sharing in cognitive radio

Digital Object Identifier 10.4316/AECE.2016.01009

networks. We transmit weighted versions of symbols over switchable weakly correlated beampatterns of the ESPAR antenna, while taking into consideration maximizing antenna efficiency. The weight vector is optimized such that it maximizes transmitted power to a SU-Rx while constraining interference to multiple PU-Rxs to be under a certain limit. As our simulations show, this achieves power performance enhancement compared to [16], while taking into consideration a more practical assumption of non-line-of-sight communication as compared to [17]. It is worth noting that the concept of assigning weights over the ESPAR antenna patterns was reported in [10] for achieving receive diversity, using a five-element ESPAR antenna. However, since their goal was to create statistically independent receive branches only, their algorithm leads to patterns with gains that are less than 3 dB. Contrarily, we optimize *maximized-gain patterns* with gains of 6.11 dB for a *three-element* ESPAR antenna to enhance the transmit power performance of the ESPAR antenna in underlay spectrum sharing paradigm. We also optimize maximized-gain patterns with gains of 7 dB for a seven-element ESPAR antenna.

The contribution of this paper can be summarized as follows. We study the power performance enhancement resulting from using a transmitter ESPAR antenna with switchable maximized-gain beampatterns in underlay spectrum sharing. We also investigate the performance of two different beampattern shapes of ESPAR antenna, and we choose the appropriate beampattern shape for underlay spectrum sharing. We show through simulation that the ESPAR antenna can offer a better power performance than a classical CAA of the same size and nearly the same number of elements. Moreover, we show that ESPAR antenna can preserve its good performance in case of small spacing between elements, whereas the classical CAA's performance severely degrades.

The rest of the paper is organized as follows. Section II describes the ESPAR antenna system model. Section III covers the wireless system model, the performance analysis of different types of beampattern shapes of the ESPAR antenna in underlay spectrum sharing paradigm, and a qualitative comparison between the proposed transmitter system and a classical CAA. Numerical performance evaluations and comparisons are given in Section IV. Section V concludes the paper.

Notation: Boldface capital letters refer to matrices and boldface small letters refer to vectors of the specified size. $<\cdot>_{x,y}$ returns the $\{x, y\}$ entry of the enclosed matrix and $<\cdot>_x$ returns the x^{th} element of the enclosed vector. $|\cdot|$ gives the magnitude of the enclosed complex number. The superscripts T, * and H denote transpose, conjugate and transpose conjugate, respectively. j is the imaginary unit ($j=\sqrt{-1}$).

II. ESPAR Antenna System Model

Consider *(K+1)* dipoles of lengths *λ/2* forming a circular ESPAR antenna array of radius *r*. The active dipole lies at the center of the circle and the remaining *K* passive dipoles lie uniformly at the circumference. *K* switchable beampatterns can be created, and the field pattern of the k^{th} beampattern in the azimuthal plane is [15]

$$B_k(\varphi)=\mathbf{i}_k^T\boldsymbol{\alpha}(\varphi), \tag{1}$$

where $k\in\{1, .., K\}$, and φ is the azimuthal angle of departure of the transmitted signal. $\boldsymbol{\alpha}(\varphi)\in\mathbb{C}^{(K+1)\times 1}$ is the steering vector of the antenna array and is defined as

$$\boldsymbol{\alpha}(\varphi)=\left[1, e^{-j\frac{2\pi r}{\lambda}\cos(\varphi)}, \ldots, e^{-j\frac{2\pi r}{\lambda}\cos(\varphi-2\pi\frac{K-1}{K})}\right]^T. \tag{2}$$

The vector $\mathbf{i}_k\in\mathbb{C}^{(K+1)\times 1}$ defines the currents in the ESPAR antenna elements where

$$\mathbf{i}_k=v_s\left[\mathbf{Z}+\mathbf{X}_k\right]^{-1}\mathbf{v}, \tag{3}$$

where v_s represents the applied voltage source signal, $\mathbf{Z}\in\mathbb{C}^{(K+1)\times(K+1)}$ is the mutual coupling impedance matrix of the ESPAR antenna and it is calculated as a function of the pairwise distances between the dipoles and the lengths of the dipoles as in [18], $\mathbf{X}_k\in\mathbb{C}^{(K+1)\times(K+1)}$ is a diagonal matrix of the vector $\mathbf{a}_k=[Z_L, j\mathbf{x}_k^T]$, Z_L is the complex load impedance on the active element, $j\mathbf{x}_k\in\mathbb{C}^{K\times 1}$ defines the reactive loads on the passive elements, and the vector $\mathbf{v}\in\mathbb{R}^{(K+1)\times 1}$ is given by $\mathbf{v}=[1,0,..,0]^T$. Switching between beampatterns can be done simply by circularly permuting physical loads of the passive elements.

The power gain of the k^{th} beampattern is given as

$$G_{p,k}(\varphi)=\eta\frac{B_k(\varphi)B_k^*(\varphi)}{\frac{1}{2\pi}\int_0^{2\pi}B_k(\varphi)B_k^*(\varphi)d\varphi}, \tag{4}$$

where $\eta\in[0, 1]$ is the antenna efficiency and is defined as

$$\eta=1-\left|\frac{z_{in}-z_L^*}{z_{in}+z_L}\right|^2, \tag{5}$$

where

$$z_{in}=\langle\mathbf{Z}\rangle_{00}+\frac{1}{\langle\mathbf{i}_k\rangle_0}\sum_{t=1}^{K}\langle\mathbf{Z}\rangle_{0t}\langle\mathbf{i}_k\rangle_t. \tag{6}$$

Also, the complex voltage gain of the k^{th} beampatterns can be calculated as

$$G_{\mathrm{v},k}(\varphi)=\sqrt{\eta}\frac{B_k(\varphi)}{\sqrt{\frac{1}{2\pi}\int_0^{2\pi}B_k(\varphi)B_k^*(\varphi)d\varphi}}. \tag{7}$$

III. Proposed ESPAR Antenna Transmitter System for Underlay Spectrum Sharing

A. Wireless System Model

We consider an underlay spectrum-sharing paradigm with a single SU-Tx, a single SU-Rx and multiple PU-Rxs. We assume a uniform power angle spectrum environment and consider a device-to-device communication between the two SUs. The SU-Tx is equipped with an ESPAR antenna, and transmits symbols to the SU-Rx, which is equipped with an

isotropic antenna, while jointly keeping interference to N PU-Rxs (equipped with isotropic antennas) under a certain limit.

The approach for transmitting the symbols is as follows. The symbols are transmitted over the switchable patterns $G_{v,k}(\varphi)$ of the ESPAR antenna. If we kept the correlation between any of the ESPAR antenna beampatterns under 0.7, the transmitted symbols over them will experience independent (or weakly-correlated) channels [19], where the correlation between two beampatterns is given by

$$\langle \mathbf{R} \rangle_{k,j} = \frac{\int_0^{2\pi} B_k(\varphi) B_j^*(\varphi) d\varphi}{\sqrt{\int_0^{2\pi} B_k(\varphi) B_k^*(\varphi) d\varphi \int_0^{2\pi} B_j(\varphi) B_j^*(\varphi) d\varphi}}. \quad (8)$$

By doing so, one can regard the ESPAR antenna switchable beampatterns as *virtual antenna array elements,* where symbols are transmitted over them while experiencing statistically independent channels. Thus, the system resembles to a single MISO channel $\mathbf{s} \in \mathbb{C}^{K\times 1}$ from the ESPAR antenna virtual antenna array elements towards the SU-Rx, and another MISO channel $\mathbf{i}_n \in \mathbb{C}^{K\times 1}$ towards the n^{th} PU-Rx; the equivalent channel model is shown in Fig. 1.

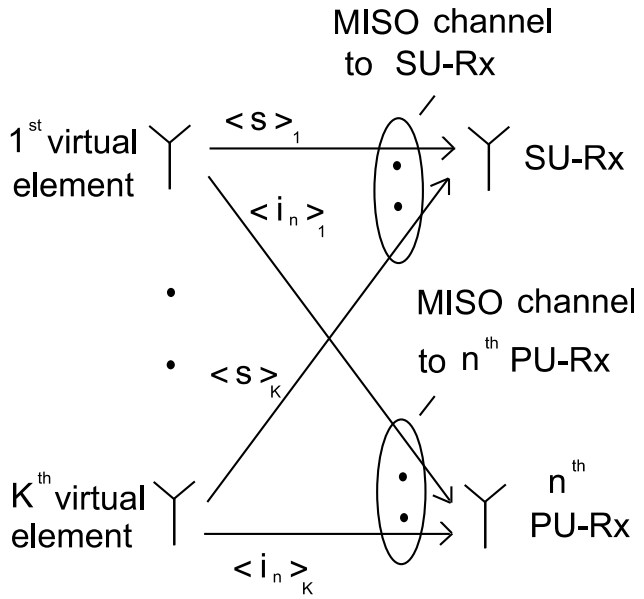

Figure 1. MISO channels created from the SU-Tx virtual antenna elements to the SU-Rx and to each of the PU-Rxs

Mathematically, the signal and interference channels, respectively, are given as follows

$$\langle \mathbf{s} \rangle_k = \sqrt{d_s^{-\alpha}} \sum_{l=1}^{L_s} s_l'(\varphi_l) G_{v,k}(\varphi_l), \quad (9)$$

$$\langle \mathbf{i}_n \rangle_k = \sqrt{d_{p,n}^{-\alpha}} \sum_{l=1}^{L_{p,n}} i_{l,n}'(\varphi_l) G_{v,k}(\varphi_l), \quad (10)$$

where d_s and $d_{p,n}$ are the distances from the SU-Tx to the SU-Rx and to the n^{th} PU-Rx, respectively, α is the path loss exponent, L_s and $L_{p,n}$ are the total number of paths from the SU-Tx to the SU-Rx and to the n^{th} PU-Rx, respectively, s_l' and $i_{l,n}'$ are the l^{th} path channel responses from the SU-Tx to the SU-Rx and the n^{th} PU-Rx, respectively, and f_l is the angle of departure of the l^{th} path.

Hence, if we transmitted weighted versions of a symbol x over the switchable beampatterns of the ESPAR antenna, the transmitted voltage signal from the ESPAR antenna can be written using Kronecker model [20] as

$$v_T = \mathbf{w}^H \mathbf{R}^{1/2} \mathbf{s} x + \sum_{n=1}^{N} \mathbf{w}^H \mathbf{R}^{1/2} \mathbf{i}_n x \quad (11)$$

where $\mathbf{w} \in \mathbb{C}^{K\times 1}$ is the precoding weight vector over the virtual antenna elements, and $\mathbf{R} \in \mathbb{C}^{K\times K}$ is the correlation matrix between the ESPAR antenna switchable beampatterns, where the matrix elements are given by (8). The precoding weight vector is optimized as follows

$$\begin{aligned} \max_{\mathbf{w}} . \quad & \left| \mathbf{w}^H \mathbf{R}^{1/2} \mathbf{s} \right|^2 \\ s.t. \quad & \left| \mathbf{w}^H \mathbf{R}^{1/2} \mathbf{i}_n \right|^2 \le \gamma, \quad \forall n \\ & \left\| \mathbf{w} \right\|^2 \le 1, \end{aligned} \quad (12)$$

where γ is the predefined interference threshold at the PU-Rxs. This problem can be considered as a Lagrangian optimization problem with inequality constraints.

In the following subsection we will study the performance of two different shapes of switchable beampatterns, and choose the beampattern shape that achieves the higher power performance. After that, we will compare the proposed transmitting system to a classical CAA of the same size and (nearly) the same number of elements.

B. Pattern Shape Optimization

We now optimize the shapes of the beampatterns of the ESPAR antenna for enhancing the performance of underlay spectrum sharing. We study two types of patterns shapes of the ESPAR antenna: maximized-gain and maximized-efficiency beampatterns. The physical loads creating a maximized-gain beampattern can be found through solving the following optimization problem

$$\begin{aligned} \max_{\mathbf{a}_1} . \quad & G_{p,1}\left(\varphi = 0^\circ\right) \\ s.t. \quad & \langle \mathbf{R} \rangle_{1,2} \le 0.7 \\ & 0 - j100 \le Z_L \le 100 + j100 \\ & -100 \le \langle \mathbf{x}_1 \rangle_y \le 100, \qquad y \in \{1,..,K\}, \end{aligned} \quad (13)$$

where we have chosen the allowable reactive loading on ESPAR elements to be in the range *[-100j, 100j]* Ω, and the allowable resistance loading on the active element to be in the range *[0, 100]* Ω. Also, we constrain the correlation between two successive beampatterns to be under 0.7, which also ensures that the correlation between any other two beampatterns to be under 0.7. This optimization problem can be solved via a constrained nonlinear optimization MATLAB routine.

On the other hand, the physical loads creating a maximized-efficiency beampattern can be found through solving the optimization problem

$$\begin{aligned} \max_{\mathbf{a}_1} .\quad & \eta \\ s.t.\quad & \langle \mathbf{R} \rangle_{1,2} \le 0.7 \\ & 0 - j100 \le Z_L \le 100 + j100 \\ & -100 \le \langle \mathbf{x}_1 \rangle_y \le 100, \qquad y \in \{1,..,K\}. \end{aligned} \tag{14}$$

It is noted that the maximized-efficiency beampatterns are optimized such that the *total radiated power* of the antenna is maximized, whereas maximized-gain beampatterns are optimized such that their power patterns are concentrated at specific angles. This makes the maximized-gain beampatterns have smaller beamwidths than maximized-efficiency beampatterns (see Fig. 2 for patterns shapes of a seven-element ESPAR antenna). As we show through simulations, the maximized-gain beampatterns are able to deliver higher power to the SU-Rx than the maximized-efficiency beampatterns. The justification for this is given as follows.

From (8), since the correlation coefficient between any two patterns depends only on the patterns shapes and the angular separation between them, the correlation matrix is a symmetric circulant matrix. This means that the square root of the correlation matrix takes the form

$$\mathbf{R}^{1/2} = \begin{bmatrix} r_1 & r_2 & r_3 & \cdots & r_3 & r_2 \\ r_2 & r_1 & r_2 & r_3 & \cdots & r_3 \\ r_3 & r_2 & \ddots & \ddots & \ddots & \vdots \\ \vdots & \ddots & \ddots & \ddots & r_2 & r_3 \\ r_3 & & \ddots & r_2 & r_1 & r_2 \\ r_2 & r_3 & \cdots & r_3 & r_2 & r_1 \end{bmatrix} = \begin{bmatrix} \mathbf{r}_1 & \cdots & \mathbf{r}_K \end{bmatrix}, \tag{15}$$

where $\boldsymbol{r}_k$ is *(K×1)* column vector whose elements are the square roots of the correlation coefficients between the K beampatterns. Let us define vectors $\mathbf{s}_R = \mathbf{R}^{1/2}\mathbf{s}$ and $\mathbf{i}_{R,n} = \mathbf{R}^{1/2}\mathbf{i}_n$. Thus, vectors $\mathbf{s}_R$ and $\mathbf{i}_{R,n}$ can be written as linear combinations of the column vectors $\boldsymbol{r}_k$ as follows

$$\mathbf{s}_R = \mathbf{R}^{1/2}\mathbf{s} = \sum_{k=1}^{K} \langle \mathbf{s} \rangle_k \, \mathbf{r}_k, \tag{16}$$

$$\mathbf{i}_{R,n} = \mathbf{R}^{1/2}\mathbf{i}_n = \sum_{k=1}^{K} \langle \mathbf{i}_n \rangle_k \, \mathbf{r}_k, \quad \forall n. \tag{17}$$

Problem (12) is ideally solved when the complex random vector $\mathbf{s}_R$ is orthogonal to the subspace spanned by the complex random vectors $\mathbf{i}_{R,n}$; so, the weight vector $\boldsymbol{w}$ is chosen in the direction of $\mathbf{s}_R$ and orthogonal to vectors $\mathbf{i}_{R,n}$. In the remainder of this section, we investigate the effect of the beamwidths of the antenna patterns on the characteristics of $\boldsymbol{r}_k$, and we show how this affects the characteristics of vectors $\mathbf{s}_R$ and $\mathbf{i}_{R,n}$ and the solution of (12).

Without loss of generality, we can model the beampattern of the ESPAR antenna as a Gaussian function of the form

$$B_k(\varphi) = e^{\frac{-(\varphi-\varphi_k)^2}{2\sigma^2}}, \quad -\pi \le \varphi - \varphi_k \le \pi \tag{18}$$

where σ is the Gaussian spread parameter and it is related to the half-power beamwidth (HPBW) of $B_k(\varphi)$ through the relation $HPBW = \sigma^2\sqrt{2\ln\sqrt{2}}$, and φ_k is the angle of maximum radiation of the k^{th} beampattern and is defined by

$$\varphi_k = 2\pi\frac{k-1}{K}. \tag{19}$$

We use (8) to calculate the correlation coefficient between the first and the k^{th} patterns. After some mathematical manipulation we find that

$$\langle \mathbf{R} \rangle_{1,k} = e^{\frac{-\varphi_k^2}{4\sigma^2}}. \tag{20}$$

This relation clearly states that the correlation coefficient between the first and the k^{th} beampatterns is exponentially decaying with the angle of maximum radiation φ_k. Moreover, narrow beamwidths result in smaller values of σ and steeper decay of $<\boldsymbol{R}>_{1,k}$ with φ_k, and vice versa. Thus, as the beamwidths becomes wider, the correlation coefficients of the matrix $\boldsymbol{R}$ become more similar to each other, which increase the correlation between the vectors $\boldsymbol{r}_k$.

Intuitively, in the case of highly correlated vectors $\boldsymbol{r}_k$, the correlation between the vectors $\mathbf{s}_R$ and $\mathbf{i}_{R,n}$ is more likely to increase, as these vectors are linear combinations of the vectors $\boldsymbol{r}_k$. This in turn leads to low power delivery to the SU-Rx. Contrarily, when the beamwidths are smaller, the vectors $\boldsymbol{r}_k$ become weakly correlated to each other, and the vectors $\mathbf{s}_R$ and $\mathbf{i}_{R,n}$ become likely to be weakly correlated, which leads to a high power delivery to the SU-Rx. This analysis explains why maximized-gain beampatterns, which attain small beamwidths, are expected to deliver higher power to the SU-Rx than the maximized-efficiency beampatterns that attain wide beamwidths. This result is validated experimentally in the next section.

C. Comparison of the Proposed Transmitter System with the Classical CAA

Having optimized the ESPAR antenna patterns for the underlay spectrum sharing paradigm, it is interesting now to compare the proposed transmitter ESPAR antenna of *(K+1)* dipoles with gain-maximized beampatterns, with a classical CAA of K dipoles. Firstly, the gain of each transmit branch of the classical CAA (the individual dipoles) is known to be 2.15 dB [21], while the transmit branches of ESPAR antenna (the switchable beampatterns) are of gains $G_0 = \max_{\varphi}(G_{p,k}(\varphi))$, which will be shown to be 7 dB for a seven-element ESPAR antenna. This normally enhances the transmitted power level. Moreover, since the ESPAR antenna is using K *switchable* beampatterns, it will need only 1/K of the power needed by the classical CAA to create its K corresponding transmit branches.

Further, an ESPAR antenna with a very small radius (for instance *λ/20*) will be still able to create weakly-correlated beampatterns, and hence, work properly. This is because the correlation between any two successive patterns in the ESPAR antenna system depends only on the patterns shapes not on the separation between the physical elements of the array as shown in (8). On the other hand, the correlation between the individual dipoles of the CAA depends on the separation between them. This correlation can be calculated from

$$\langle \mathbf{R} \rangle_{x,y} = \frac{1}{2\pi} \int_{-\pi}^{\pi} e^{j\frac{2\pi}{\lambda} d_{x,y} \cos(\varphi)} d\varphi, \quad (21)$$

where $d_{x,y}$ is the distance between the x^{th} and y^{th} elements. As shown earlier, higher correlation between transmit branches results in less power delivered to SU-Rx. Hence, the performance of the classical CAA of very small radiuses degrades severely. Section IV presents numerical evaluation of correlation and power performance of small-radius CAA.

IV. Performance Evaluation

For our proposed system performance evaluation, we consider a seven-dipole circular ESPAR antenna of radius $\lambda/4$ as a transmitter unless otherwise stated. For simplicity, we assume equal distances from the SU-Tx to the SU-Rx and to all PU-Rxs, i.e. $d = d_s = d_{p,n}, \forall n$. The path loss exponent α is taken as 2, φ_l is modeled as a uniformly-distributed random variable as we are assuming a uniform power angle spectrum environment, $s_l^{'}$ and $i_{l,n}^{'}$ are modeled as Rayleigh-distributed random variables with zero means and unit variances unless stated otherwise, and γ is taken as 1 μW. The transmitted power to the SU-Rx is averaged over 1000 randomly-generated channel responses.

The optimization problems of (13) and (14) are solved using constrained nonlinear optimization MATLAB routine to find the optimum physical loads. The achieved efficiency in the two problems is found to be $\eta=1$, and one pattern of each type is plotted in Fig. 2.

The correlation matrix in the maximized-gain beampatterns case is found to be

$$\mathbf{R} = \begin{bmatrix} 1 & 0.313 & 0.216 & 0.427 & 0.216 & 0.313 \\ 0.313 & 1 & 0.313 & 0.216 & 0.427 & 0.216 \\ 0.216 & 0.313 & 1 & 0.313 & 0.216 & 0.427 \\ 0.427 & 0.216 & 0.313 & 1 & 0.313 & 0.216 \\ 0.216 & 0.427 & 0.216 & 0.313 & 1 & 0.313 \\ 0.313 & 0.216 & 0.427 & 0.216 & 0.313 & 1 \end{bmatrix}. \quad (22)$$

After taking the square root of this matrix, we calculate the correlation between all the matrix columns and the average correlation between them is found to be 0.903. The correlation matrix in the maximized-efficiency beampatterns case is found to be

$$\mathbf{R} = \begin{bmatrix} 1 & 0.603 & 0.380 & 0.424 & 0.380 & 0.603 \\ 0.603 & 1 & 0.603 & 0.380 & 0.424 & 0.380 \\ 0.380 & 0.603 & 1 & 0.603 & 0.380 & 0.424 \\ 0.424 & 0.380 & 0.603 & 1 & 0.603 & 0.380 \\ 0.380 & 0.424 & 0.380 & 0.603 & 1 & 0.603 \\ 0.603 & 0.380 & 0.424 & 0.380 & 0.603 & 1 \end{bmatrix}. \quad (23)$$

And again, after taking the square root of this matrix, we calculate the correlation between all the matrix columns and the average correlation between them is found to be 0.962. This shows the lower correlation between vectors $\mathbf{r}_k$ in case of maximized-gain beampatterns, which results in higher power delivered than the maximized-efficiency beampatterns case.

A. Maximized-Gain versus Maximized-Efficiency Beampatterns

We compare between two ESPAR antennas with maximized-gain beampatterns and maximized-efficiency beampatterns, each with $\lambda/4$ radius, in order to find the optimum weight vector in (12). The transmitted power to a SU-Rx at different distances in cases of one PU-Rx and four PU-Rxs is calculated and shown in Fig. 3. Generally, it is noticed that maximized-gain beampatterns deliver higher power to the SU-Rx than maximized-efficiency beampatterns. We also note that the larger the number of PU-Rxs, the lower the transmitted power to SU-Rx. This is attributed to the fact that increasing the number of PU-Rxs increases the number of vectors $\mathbf{i}_{R,n}$, and the interference constraints of (12) have to be satisfied for the most correlated vector $\mathbf{i}_{R,n}, \forall n$ to $\mathbf{s}_R$.

The interference signal at each PU-Rx is also calculated, and it is found to be equal to the predefined interference threshold, which is 1 μW.

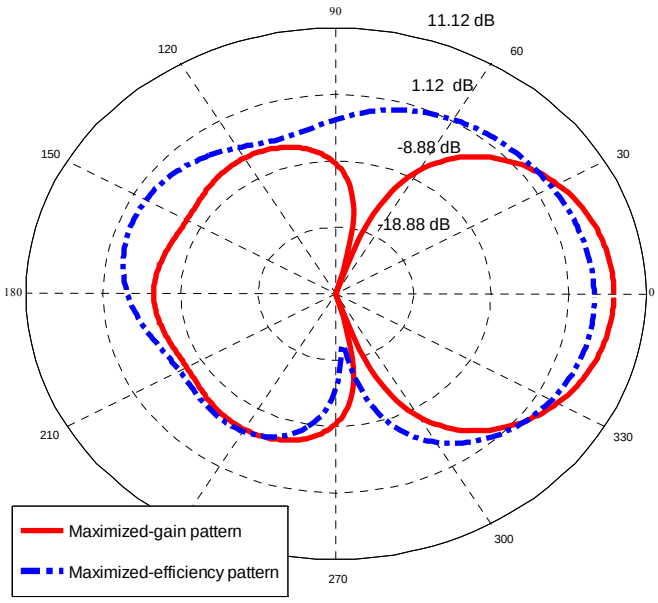

Figure 2. One of the six maximized-gain beampatterns, and one of the six maximized-efficiency beampatterns are shown for a seven-element ESPAR antenna

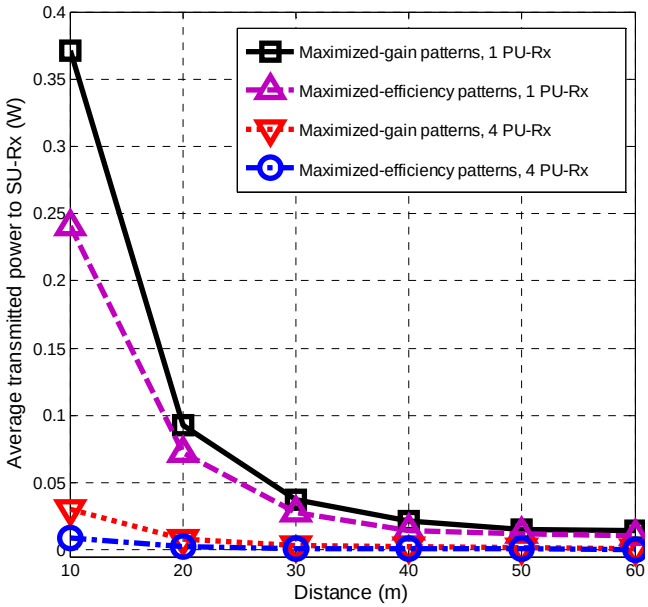

Figure 3. Average transmitted power to the SU-Rx in case of maximized-gain and maximized- efficiency patterns, number of PU-Rxs equal to 1 and 4

B. Comparison Between the Proposed ESPAR Antenna System and the Classical CAA

We compare the proposed ESPAR antenna system with a classical CAA of $\lambda/4$ radiuses as transmitters to solve the problem (12), and we apply an equal total source power to both of them. The power transmitted to the SU-Rx in the two cases is shown in Fig. 4, for different distances. ESPAR antenna is shown to achieve superior performance, as the power of each transmit branch in the ESPAR antenna is six times higher than the classical CAA, as discussed earlier.

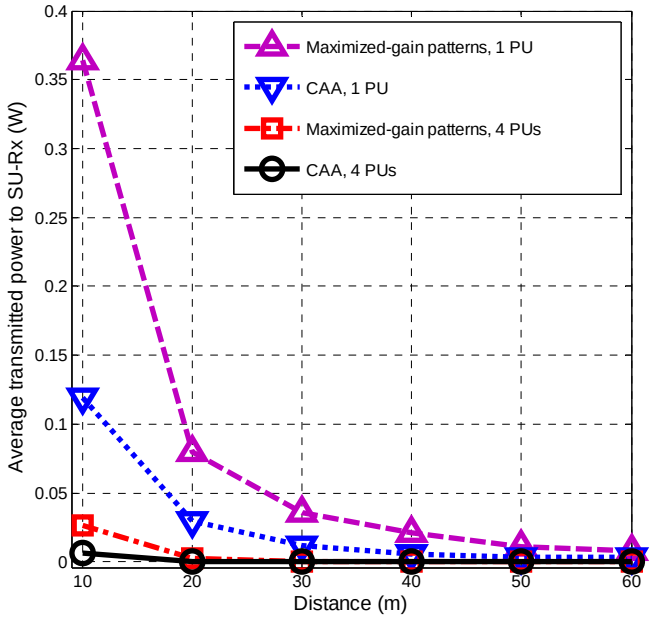

Figure 4. Average transmitted power to the SU-Rx in case of maximized-gain ESPAR patterns and CAA, for r=λ/4, number of PU-Rxs equal to 1 and 4

We again compare the same types of transmitter antennas but of radiuses λ/20. In this case, in addition to the higher power of transmit branches in ESPAR antenna, the high correlation between the transmit branches of the CAA severely degrades its performance compared to the ESPAR antenna. This result is shown in Fig. 5. It can be noted that the power performance of the ESPAR antenna coexisting with four PU-Rxs is better than the power performance of the CAA coexisting with only one PU-Rx.

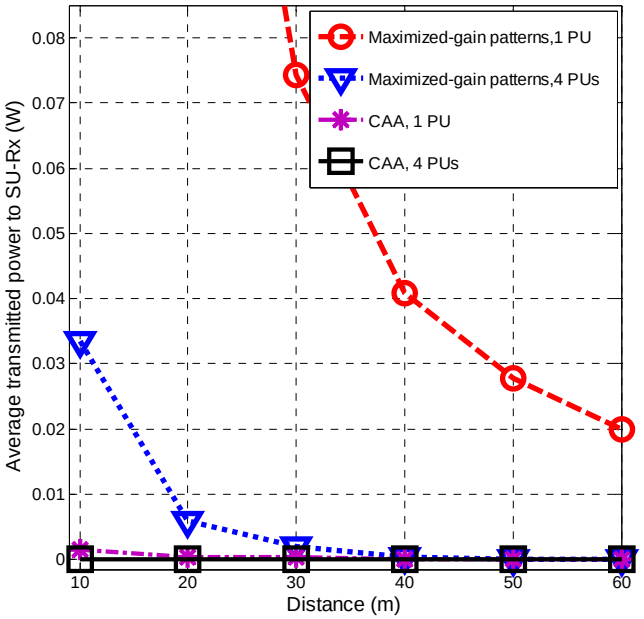

Figure 5. Average transmitted power to the SU-Rx in case of maximized-gain ESPAR patterns and CAA, for r=λ/20, number of PU-Rxs equal to1 and 4

It is interesting to note that even if we set the input power to the classical CAA of radius $\lambda/20$ to be six times higher than the ESPAR antenna of radius $\lambda/20$, the ESPAR antenna would still be able to transmit higher power to the SU-Rx, as shown in Fig. 6. Again, this is because of the high correlation between the transmit branches of the classical CAA, which severely degrades its performance.

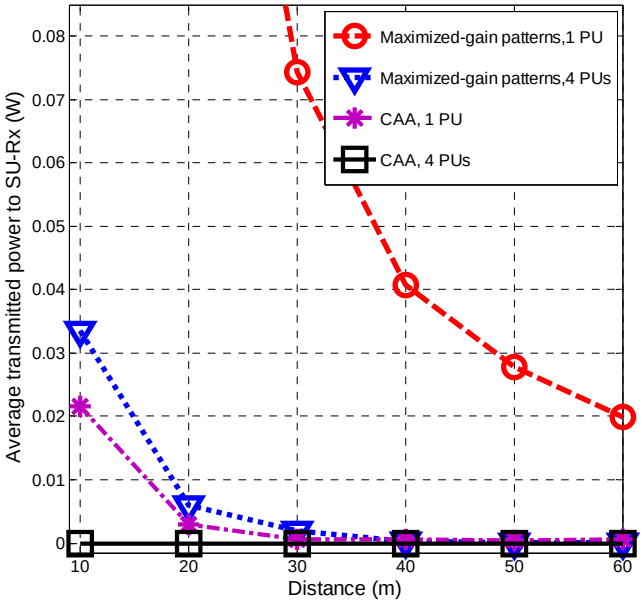

Figure 6. Average transmitted power to the SU-Rx in case of maximized-gain ESPAR patterns and CAA, for $r=\lambda/20$, , number of PU-Rxs equal to 1 and 4, and assuming an input power to the classical CAA that is six times higher than the input power to the ESPAR antenna

C. Performance Comparison with Orthogonal Precoding Algorithm [16]

In [16], a linear combination of linearly independent patterns or basis is used such that the resultant pattern forms nulls towards the PU-Rxs. However, the proposed approach

did not maximize antenna efficiency, which can considerably affect the power performance of the antenna. Moreover, it did not pay attention to maximizing the transmitted power to the SU-Rx, which is important specifically in stationary networks.

On the other hand, our proposed algorithm maximizes the antenna efficiency. Moreover, it chooses the optimum precoding weight vector over virtual antenna elements to maximize the transmitted power to the SU-Rx while constraining the interference to PU-Rx.

To begin comparison, we consider the following scenario. A PU-Rx located at 120 degrees with respect to the SU-Tx, and the angle of the SU-Rx with respect to the SU-Tx is a variable. We also consider a line-of-sight communication, a Rician fading channel with unity standard deviation, and a three-dipole ESPAR antenna as a transmitter (for a fair comparison with [16]). Using the orthogonal precoding algorithm of [16], the resultant power pattern is shown in Fig. 7a irrespectively of the direction of the SU-Rx. We use this power pattern to calculate the average transmitted power to SU-Rx at different directions. The results are shown in Fig. 8.

On the other hand, the switchable maximized-gain power patterns using the proposed algorithm are shown in Fig. 7b. We first place the SU-Rx at 0 degree and calculate the optimum weight vector in problem (12). The average transmitted power to the SU-Rx is calculated. Then, we repeat the previous steps for SU-Rx at different directions. The results are also shown in Fig. 8, and clearly show superior performance for our proposed approach. The justification of the superiority of our algorithm is as follows.

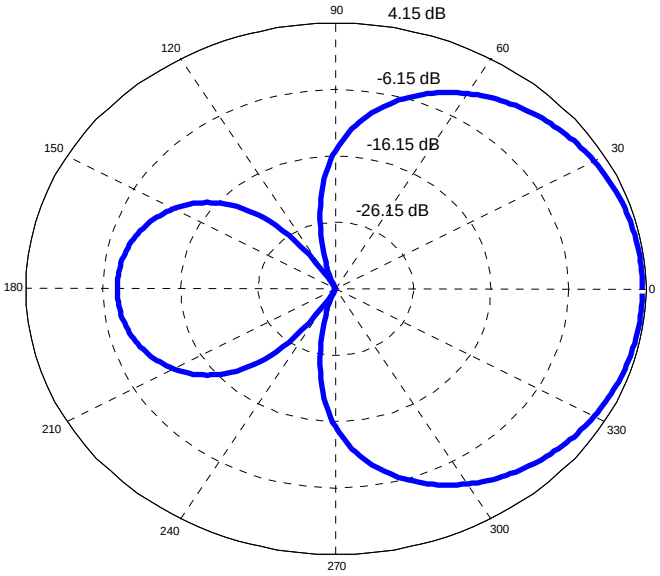

(a)

Generally, the maximized efficiency of the antenna in our proposed system leads to power patterns with higher gains than the orthogonal precoding algorithm, as shown in Fig. 7. The gain of each switchable beampattern of our proposed system is 6.11 dB, whereas it is only 3.69 dB for the orthogonal precoding algorithm. This helps to deliver more power to the SU-Rx Rx in more directions as compared to the orthogonal precoding algorithm. Also, as seen from Fig. 8, the high power delivery to the SU-Rx at most directions implies that our proposed algorithm is able to find the optimum weight vector $\boldsymbol{w}$ that is highly correlated to the vector $\mathbf{s}_R$ and weakly correlated to the vector $\mathbf{i}_{R,1}$.

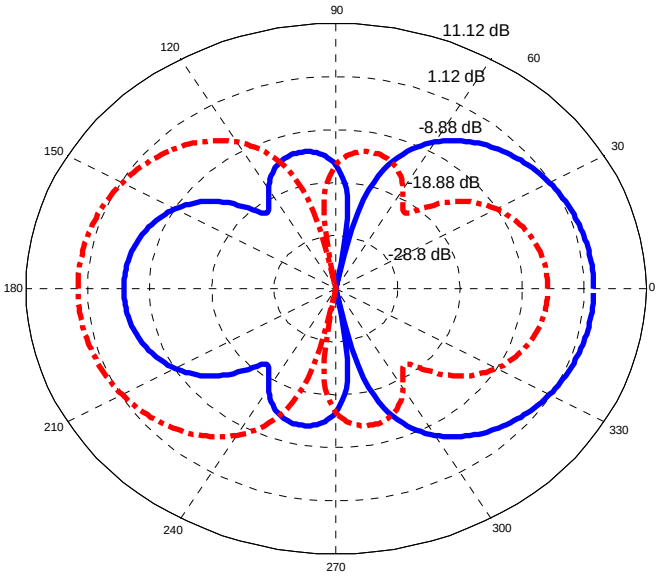

(b)

Figure 7. (a) Power pattern generated by [16] to transmit a null towards a PU-Rx at the direction of 120 degree, (b) The two switchable maximized-gain beampatterns of a three dipoles ESPAR antenna

Furthermore, we show in Fig. 9 a plot of the average transmitted power to the SU-Rx at 0 degree at different values of the interference threshold in decibels. It can be seen that our proposed algorithm delivers higher power to the SU-Rx at different interference threshold values. Also, we plot in Fig. 9 the interference at the PU-Rx using each algorithm. As shown, for different values of the interference threshold, our proposed algorithm is able to maintain the interference at the PU-Rx under the interference threshold. On the other hand, the orthogonal precoding algorithm cannot reduce the induced interference power at the PU-Rx below *-46.49* dBW.

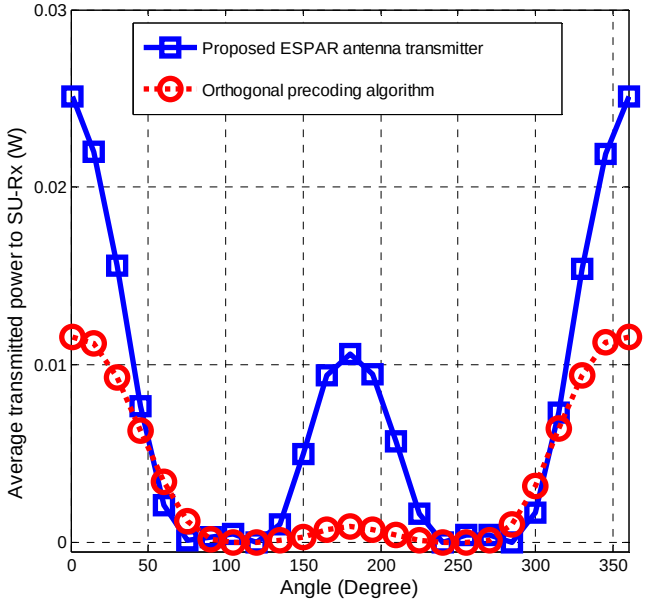

Figure 8. Average transmitted power to SU-Rx located at different angular directions for our proposed algorithm and the orthogonal precoding algorithm [16]. Random Rician faded channels are assumed between the SU-Tx and both SU-Rx and PU-Rx

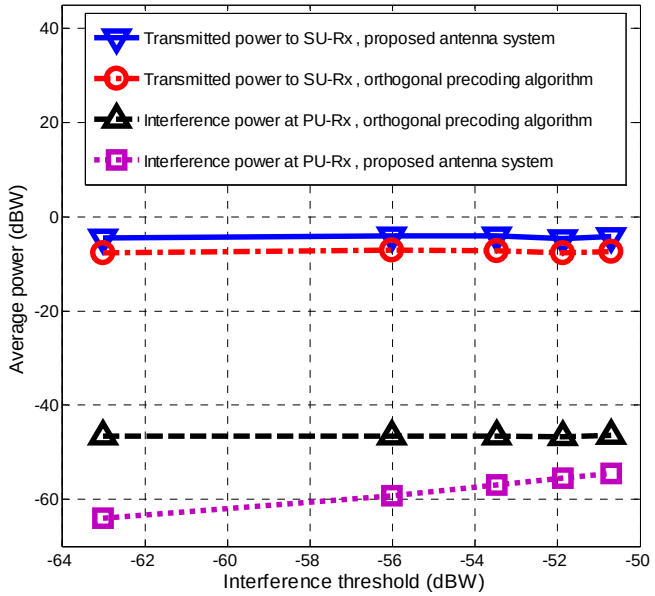

Figure 9. Average transmitted power to the SU-Rx is shown in decibels, for both cases of our proposed algorithm and the orthogonal precoding algorithm [16]. Also, the interference power at the PU-Rx is shown for the two cases

V. Conclusion

In this paper, we proposed a transmitter ESPAR antenna system for enhancing power performance in underlay spectrum sharing paradigm. We have discussed the choice of the appropriate pattern shape of the antenna. We have experimentally demonstrated the superiority of the proposed system over the orthogonal precoding algorithm and the classical circular antenna array. Using the ESPAR antenna does not only enhance the power performance, but also reduces the antenna size, cost, and complexity, which enhances the performance of underlay spectrum sharing.

References

[1] Beibei Wang and K. J. R. Liu, "Advances in cognitive radio networks: A survey," IEEE Journal of Selected Topics in Signal Processing, vol. 5, no. 1, pp. 5–23, Feb. 2011. doi: 10.1109/JSTSP.2010.2093210

[2] S. Yiu, M. Vu, and V. Tarokh, "Interference Reduction by Beamforming in Cognitive Networks," 2008, pp. 1–6. doi:10.1109/GLOCOM.2008.ECP.845

[3] L. Zhang, Y.-C. Liang, and Y. Xin, "Joint Beamforming and Power Allocation for Multiple Access Channels in Cognitive Radio Networks," IEEE Journal on Selected Areas in Communications, vol. 26, no. 1, pp. 38–51, Jan. 2008. doi:10.1109/JSAC.2008.080105

[4] V. Rakovic, D. Denkovski, and L. Gavrilovska, "Combined beamforming design for underlay spectrum sharing," 2014, pp. 58–63. doi:10.1109/WCNCW.2014.6934861

[5] L. C. Godara, "Applications of antenna arrays to mobile communications. I. Performance improvement, feasibility, and system considerations," Proceedings of the IEEE, vol. 85, no. 7, pp. 1031–1060, Jul. 1997. doi:10.1109/5.611108

[6] K. Gyoda and T. Ohira, "Design of electronically steerable passive array radiator (ESPAR) antennas," 2000, vol. 2, pp. 922–925. doi:10.1109/aps.2000.875370

[7] M. R. Islam and M. Ali, "Elevation Plane Beam Scanning of a Novel Parasitic Array Radiator Antenna for 1900 MHz Mobile Handheld Terminals," IEEE Transactions on Antennas and Propagation, vol. 58, no. 10, pp. 3344–3352, Oct. 2010. doi:10.1109/TAP.2010.2055798

[8] Q. T. Tran, Y. NAKAYA, I. Ichirou, and Y. OISHI, "An adaptive beamforming method for phased array antenna with MEMS phase shifters," IEICE transactions on communications, vol. 89, pp. 2503-2513, 2006. doi:10.1093/ietcom/e89-b.9.2503

[9] E. P. Tsakalaki, O. N. Alrabadi, C. B. Papadias, and R. Prasad, "Enhanced selection combining for compact single RF user terminals in multiuser diversity systems," 2010, pp. 951–954. doi:10.1109/PIMRC.2010.5671767

[10] V. Barousis, A. Kanatas, N. Skentos, and A. Kalis, "Pattern diversity for single RF user terminals in multiuser environments," IEEE Communications Letters, vol. 14, no. 2, pp. 151–153, Feb. 2010. doi:10.1109/LCOMM.2010.02.091941

[11] C. Sun, A. Hirata, T. Ohira, and N. C. Karmakar, "Fast Beamforming of Electronically Steerable Parasitic Array Radiator Antennas: Theory and Experiment," IEEE Transactions on Antennas and Propagation, vol. 52, no. 7, pp. 1819–1832, Jul. 2004. doi:10.1109/TAP.2004.831314

[12] R. Qian, M. Sellathurai, and D. Wilcox, "A Study on MVDR Beamforming Applied to an ESPAR Antenna," IEEE Signal Processing Letters, vol. 22, no. 1, pp. 67–70, Jan. 2015. doi:10.1109/LSP.2014.2349574

[13] V. Barousis, A. G. Kanatas, A. Kalis, and C. Papadias, "A Stochastic Beamforming Algorithm for ESPAR Antennas," IEEE Antennas and Wireless Propagation Letters, vol. 7, pp. 745–748, 2008. doi:10.1109/LAWP.2008.2004783

[14] R. Qian, M. Sellathurai, and T. Ratnarajah, "Directional spectrum sensing for cognitive radio using ESPAR arrays with a single RF chain," in Networks and Communications (EuCNC), 2014 European Conference on, 2014, pp. 1-5. doi:10.1109/eucnc.2014.6882639

[15] E. P. Tsakalaki, D. Wilcox, E. De Carvalho, C. B. Papadias, and T. Ratnarajah, "Spectrum sensing using single-radio switched-beam antenna systems," in Cognitive Radio Oriented Wireless Networks and Communications (CROWNCOM), 2012 7th International ICST Conference on, 2012, pp. 118-123. doi:10.4108/icst.crowncom.2012.248729

[16] E. P. Tsakalaki, O. N. Alrabadi, and C. B. Papadias, "Analogue orthogonal precoding using reduced-complexity transceivers," in Antennas and Propagation (APSURSI), 2011 IEEE International Symposium on, 2011, pp. 2845-2848. doi:10.1109/APS.2011.5997119

[17] D. Wilcox, E. Tsakalaki, A. Kortun, T. Ratnarajah, C. B. Papadias, and M. Sellathurai, "On Spatial Domain Cognitive Radio Using Single-Radio Parasitic Antenna Arrays," IEEE Journal on Selected Areas in Communications, vol. 31, no. 3, pp. 571–580, Mar. 2013. doi:10.1109/JSAC.2013.130321

[18] Orfanidis, J. Sophocles, Electromagnetic waves and antennas. New Brunswick, NJ: Rutgers University, pp. 916–921, 2010.

[19] R. G. Vaughan and J. B. Andersen, "Antenna diversity in mobile communications," IEEE Transactions on Vehicular Technology, vol. 36, no. 4, pp. 149–172, Nov. 1987. doi:10.1109/T-VT.1987.24115

[20] Da-Shan Shiu, G. J. Foschini, M. J. Gans, and J. M. Kahn, "Fading correlation and its effect on the capacity of multielement antenna systems," IEEE Transactions on Communications, vol. 48, no. 3, pp. 502–513, Mar. 2000. doi:10.1109/26.837052

[21] W. L. Stutzman, "Estimating directivity and gain of antennas," IEEE Antennas and Propagation Magazine, vol. 40, no. 4, pp. 7–11, Aug. 1998. doi:10.1109/74.730532